

Alkynyl and halogen Co-protected (AuAg)₄₄ Nanoclusters: A Comparative Study on Optical Absorbance, Structure Analysis, and Hydrogen Evolution Performance

Yun Tang,^a Fang Sun,^b Xiaoshuang Ma,^a Lubing Qin,^a Guanyu Ma,^a Qing Tang,^b and Zhenghua Tang^{*,a}

^aGuangzhou Key Laboratory for Surface Chemistry of Energy Materials and New Energy Research Institute, School of Environment and Energy, South China University of Technology, Guangzhou Higher Education Mega Centre, Guangzhou, Guangdong, 510006, China

E-mail: zhht@scut.edu.cn

^bSchool of Chemistry and Chemical Engineering, Chongqing Key Laboratory of Theoretical and Computational Chemistry Chongqing University, Chongqing, 401331, China

Experimental Procedures

I. Synthesis

II. Measurements and instrumentation

III. X-ray crystallography

IV. Hydrogen evolution reaction (HER) performance test

V. Computational details

Supporting Figures

Figure S1. The MALDI-TOF-MS spectra of NC 1.

Figure S2. TGA curve of NC 1.

Figure S3. The MALDI-TOF-MS spectra of NC 2.

Figure S4. TGA curve of NC 2.

Figure S5. The binding motifs of surface “Bu-PhC≡C-Au-C≡CPh-Bu” staple units of NC 1.

Figure S6. The binding motifs of surface “Bu-PhC≡C-Au-C≡CPh-Bu” staple units of NC 2.

Figure S7. The optical absorption of NC 1 with X axis plotted as energy.

Figure S8. The optical absorption of NC 2 with X axis plotted as energy.

Figure S9. The enlargement of HER polarization curves of (a) NC 1 and (b) NC 2 catalysts before and after 100 circles of scan.

Figure S10. The absorbance spectra comparison of (a) NC 1 and (b) NC 2 before and after electrochemical test.

Figure S11. CV curves of NC 1 between 0.08 and 0.18 V vs. RHE with different scan rates.

Figure S12. CV curves of NC 2 between 0.08 and 0.18 V vs. RHE with different scan rates.

Figure S13. The dependence of capacitive current and scan rate.

Figure S14. Adsorption structures of *H on NC 1 and NC 2.

Supporting Tables

Table S1. The crystal structure parameters for NC 1.

Table S2. The crystal structure parameters for NC 2.

Materials and Reagents:

Dichloromethane (DCM), dimethyl formamide (DMF), ethanol (EtOH), and methanol (MeOH) were purchased from Caiyunfei Chemical Reagents (Tianjin, China). 4-tert-butylphenylacetylene ($\text{tBuPh-C}\equiv\text{CH}$, purity: 96%), 3, 3-dimethyl-1-butyne ($\text{tBuC}\equiv\text{CH}$, purity: 96%), tetrachloroauric (III) acid ($\text{HAuCl}_4\cdot 3\text{H}_2\text{O}$, purity: 99%), anhydrous dimethyl sulfide (Me_2S , purity: 99.0%), anhydrous triethylamine (Et_3N , purity: 99.5%) were acquired from Energy Chemicals (Shanghai, China). Silver acetate (CH_3COOAg , purity: 98%), tetraphenylphosphonium bromide (PPh_4Br , purity: 98%), sodium methoxide (CH_3ONa , purity: 99%), borane-tert-butylamine complex [$(\text{CH}_3)_3\text{CNH}_2\cdot\text{BH}_3$, purity: 97%] were obtained from Aladdin Industrial Corporation (Shanghai, China). The water with the resistivity of $18.3\text{ M}\Omega\cdot\text{cm}^{-1}$ was supplied by a Barnstead Nanopure water system. All chemicals were used as received without further purification.

Synthesis of AuSMe_2Cl :

AuSMe_2Cl was prepared by following the previous report with slight modification.¹ Briefly, under Ar atmosphere, $\text{HAuCl}_4\cdot 3\text{H}_2\text{O}$ (1.00 g, 2.94 mmol) was first dissolved in anhydrous ethanol (20 mL), then a solution of Me_2S (0.65 mL, 8.82 mmol) in anhydrous ethanol (30 mL) was added directly under vigorous stirring. White precipitates began to form. The reaction mixture was kept stirring at room temperature for about 2 h until the aqueous phase became colorless. The solution was cooled to $0\text{ }^\circ\text{C}$ for 10 min, and the white precipitate were collected by filtration, washing with cold ethanol ($3 \times 10\text{ mL}$) and dry diethyl ether ($3 \times 10\text{ mL}$). The product was a white solid without drying (yield: ~95%).

Synthesis of $\text{Au}_{24}\text{Ag}_{20}(\text{tBuPh-C}\equiv\text{C})_{24}\text{Cl}_2$ nanocluster (NC 1):

In a typical synthesis, 12 mg of AuSMe_2Cl and 10 mg of CH_3COOAg were first co-dissolved in the mixed solvents of DCM and MeOH ($v: v = 2: 1$). The mixture was then cooled to $0\text{ }^\circ\text{C}$ in an ice bath and kept stirring for 5 min. Then, 40 μL of anhydrous triethylamine and 20 μL of 4-tert-butylphenylacetylene in 1 mL of methanol was introduced into the mixture under vigorous stirring. After 10 min of stirring, 7.2 mg of tert-butylamineborane dissolved in 2 mL of dichloromethane was added dropwise with a speed of $8\text{ mL}\cdot\text{h}^{-1}$. The solution was kept in ice bath for another 12 h. After that, the solvent in the organic phase was removed through rotary evaporation, then the product was washed with methanol 3 times and dissolved in toluene. After diffusion of acetonitrile into toluene at $4\text{ }^\circ\text{C}$ for about two weeks, black block crystal was obtained (yield: ~20%).

Synthesis of $\text{Au}_{22}\text{Ag}_{22}(\text{tBuC}\equiv\text{C})_{16}\text{Br}_{3.28}\text{Cl}_{2.72}$ nanocluster (NC 2):

In a typical synthesis, 12 mg of AuSMe_2Cl was first dissolved in the mixed solvents of DMF and MeOH ($v: v = 2: 1$) and 10 mg of CH_3COOAg in 2 mL DMF was then added in. The mixture was subsequently cooled to $0\text{ }^\circ\text{C}$ in an ice bath and kept stirring for 5 min. Then 1 mL of 10 mg sodium methoxide in methanol and 8 μL of 3, 3-dimethyl-1-butyne was introduced into the mixture under vigorous stirring. After 10 min of stirring, reddish clear solution was obtained and 3.6 mg of tert-butylamineborane dissolved in 1 mL of DMF was added dropwise with a speed of $6\text{ mL}\cdot\text{h}^{-1}$. Then, the reaction mixture was transferred from ice bath to room temperature for another 12 h in the absence of light. After that, the organic phase was washed with water and dichloromethane several times. The solid and aqueous phase of the mixture was discarded. The solvent organic phase was removed through rotary evaporation. The residual solid was washed with methanol 4 times and then

dissolved in dichloromethane. The above solution containing NC 2 was placed at 4 °C in a refrigerator, after slow diffusion of acetonitrile into dichloromethane solvent for around a week, black rhombic crystals were obtained (yield: ~15.2%).

II. Measurements.

UV-visible (UV-Vis) absorption spectra was recorded on a Shimadzu 2600/2700 spectrophotometer (Japan) using a quartz cuvette of 1 mm path length. Mass spectrum was recorded on a Bruker MALDI-TOF-MS with trans-2-[3-(4-tert-Butylphenyl)-2-methyl-2-propenylidene] malononitrile (DCTB) as a matrix. Thermogravimetric Analysis was performed on a NETZSCH STA 449 F5 machine during the temperature of RT to 900 °C.

III. Single Crystal Analysis.

Data collection for $\text{Au}_{24}\text{Ag}_{20}(\text{tBuPh-C}\equiv\text{C})_{24}\text{Cl}_2$ and $\text{Au}_{22}\text{Ag}_{22}(\text{tBuC}\equiv\text{C})_{16}\text{Br}_{3.28}\text{Cl}_{2.72}$ were carried on an Agilent Technologies Super Nova Single Crystal Diffractometer using MoK_α radiation ($\lambda = 0.71073 \text{ \AA}$) at 100 K and at 149.99 K, respectively. Absorption corrections were applied by using the program CrysAlis (multi-scan). Structure solution was carried out using SHELXT and refinement with SHELXL, within the OLEX2 graphical interface. All non-hydrogen atoms were refined first isotropically and then anisotropically. All the hydrogen atoms of the ligands were placed in calculated positions with fixed isotropic thermal parameters and included in the structure factor calculations in the final stage of full-matrix least-squares refinement. Detailed crystal data and structure refinements for the molecule are given in Table S1 and Table S2. CCDC number of 2159664 and 2129048 for $\text{Au}_{24}\text{Ag}_{20}(\text{tBuPh-C}\equiv\text{C})_{24}\text{Cl}_2$ and $\text{Au}_{22}\text{Ag}_{22}(\text{tBuC}\equiv\text{C})_{16}\text{Br}_{3.28}\text{Cl}_{2.72}$ contain the supplementary crystallographic data for this paper. These data are provided free of charge by the Cambridge Crystallographic Data Centre.

IV. Hydrogen evolution reaction (HER) performance test

The electrochemical tests were carried out on a CHI750 electrochemical station using a three-electrode system with a glassy carbon electrode as working electrode, a carbon rod and Ag/AgCl electrode (saturated KCl) were used as the counter and reference electrodes, respectively. The catalyst ink is prepared through the following steps: (1) 5 mg of nanoclusters were dissolved in DCM, followed by adding equivalent amount of carbon nanotube, and kept stirring for 30 min. (2) The solvent in the organic phase was removed by rotary evaporation slowly. (3) Adding 1 mL of methanol into the solids acquired in step 2) and then subjected it to ultrasonic vibration for about 30 min to ensure well dispersion. To prepare the working electrode, the ink was transferred onto the GC working electrode (catalyst loading of $\sim 0.2 \text{ mg}\cdot\text{cm}^{-2}$), followed by adding 5 μL of 0.02 wt.% Nafion (diluted from 5 wt.% Nafion, Sigma-Aldrich). The electrolyte (0.5 M H_2SO_4) was degassed by bubbling N_2 for 30 min before the electrochemical tests. The polarization curves were obtained by sweeping the potential from 0 to -0.8 V versus Ag/AgCl at room temperature with a sweep rate of $5 \text{ mV}\cdot\text{s}^{-1}$ at a rotation rate of 1000 rpm. All the data were recorded without iR correction.

V. Computational details

All the spin-polarized density functional theory (DFT) calculations were performed via using the Vienna ab initio simulation package (VASP5.4.4).² To save the computational cost, we simplified the $-\text{C}\equiv\text{C}-\text{tBu}$ and $-\text{C}\equiv\text{CPh}-\text{tBu}$ groups with $-\text{C}\equiv\text{C}-\text{CH}_3$ groups. These nanoclusters were placed in a

cubic box with dimension of $25 \text{ \AA} \times 25 \text{ \AA} \times 25 \text{ \AA}$, and their structures were optimized by the Perdew-Burke-Ernzerhof (PBE) function form of the generalized gradient approximation (GGA) to represent the interactions of exchange- correlation function.³ The ion-electron interaction was expressed by the projector augmented wave (PAW) method,⁴ and the wave functions of all the computations were expanded via a plane-wave cutoff energy of 400 eV. The convergence criteria for energy and force were 10^{-5} eV and 0.02 eV \AA^{-1} for maximal displacement, respectively. The Γ point only was used to sample the Brillouin zone, in addition, the van der Waals interactions between ligands were considered and described utilizing the empirical density functional dispersion (DFT-D3) method.⁵ All atoms were unconstrained and fully relaxed during the simulation.

The change of Gibbs free energy for HER can be calculated as:

$$\Delta G_{H^*} = \Delta E_{H^*} + \Delta ZPE - T\Delta S \quad (1)$$

Where ΔE_{H^*} is the difference in the electronic energy of hydrogen adsorption as defined as eq 2. ΔZPE is the difference of zero-point energy calculated from the vibrational frequencies, and ΔS is the entropy corrections at 298.15 K.

$$\Delta E_{H^*} = E_{M_{44} + H^*} - E_{M_{44}} - 1/2E_{H_2} \quad (2)$$

$E_{M_{44} + H^*}$, $E_{M_{44}}$, and E_{H_2} refer to the total energies of M_{44} with adsorbed H, the energy of M_{44} , and the energy of free H_2 gas, respectively.

$$\Delta S \approx -1/2S_{H_2} \quad (3)$$

Here, S_{H_2} denotes the entropy of hydrogen under standard conditions.

References

- 1 T. N. Hooper, C. P. Butts, M. Green, M. F. Haddow, J. E. McGrady and C. A. Russell, *Chem. Eur. J.*, 2009, 15, 12196-12200.
- 2 G. Kresse and J. Furthmüller, *Phys. Rev. B*, 1996, 54, 11169-11186.
- 3 J. P. Perdew, K. Burke and M. Ernzerhof, *Phys. Rev. Lett.*, 1996, 77, 3865-3868.
- 4 P. E. Blöchl, *Phys. Rev. B*, 1994, 50, 17953-17979.
- 5 I. L. Garzón and A. Posada-Amarillas, *Phys. Rev. B*, 1996, **54**, 11796-11802.

Supporting Figures

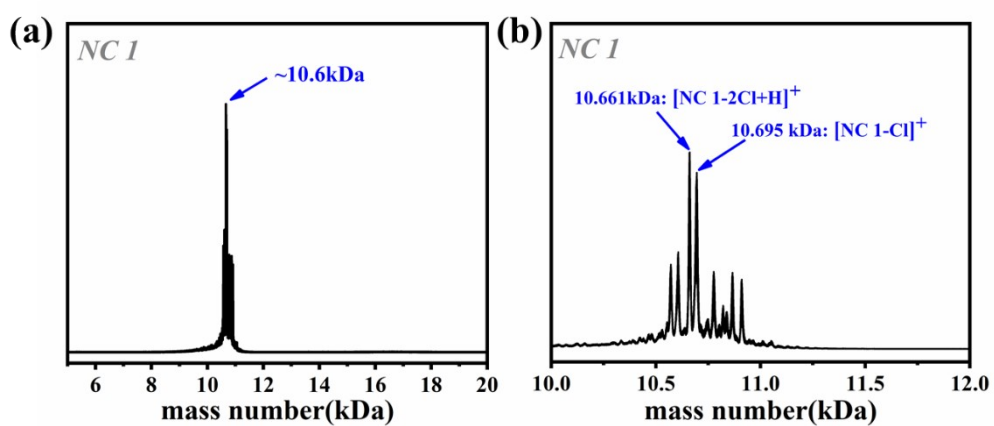


Figure S1. (a) The MALDI-TOF-MS spectra of NC 1 and (b) the enlargement of 10 kDa and 12 kDa region.

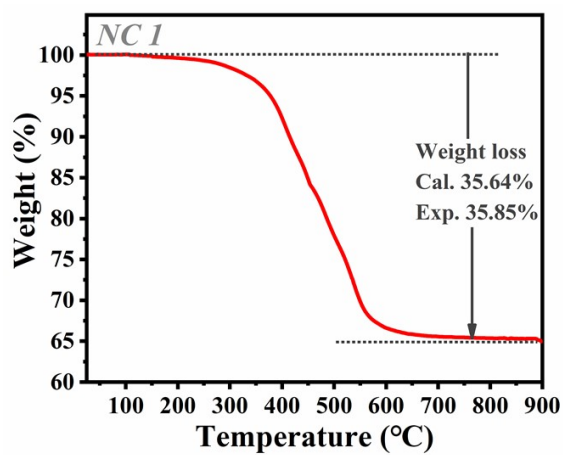


Figure S2. TGA curve of NC 1.

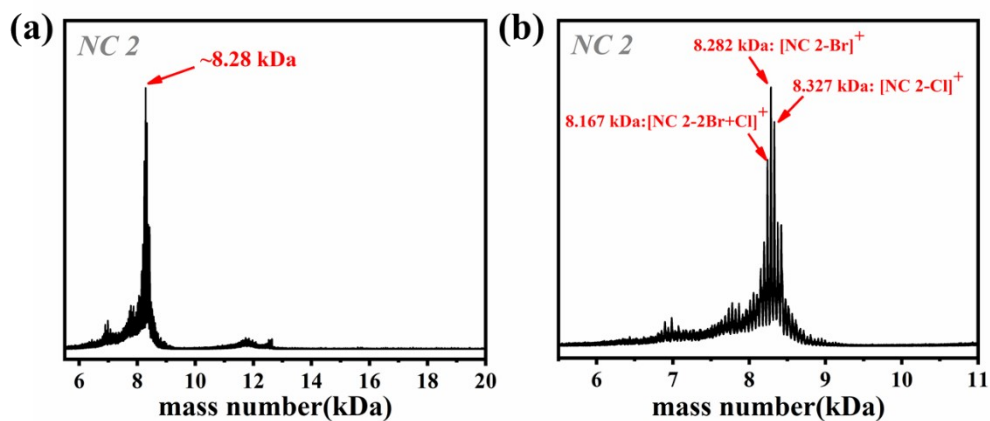


Figure S3. (a) The MALDI-TOF-MS spectra of NC 2 and (b) the enlargement of 6 kDa and 11 kDa region.

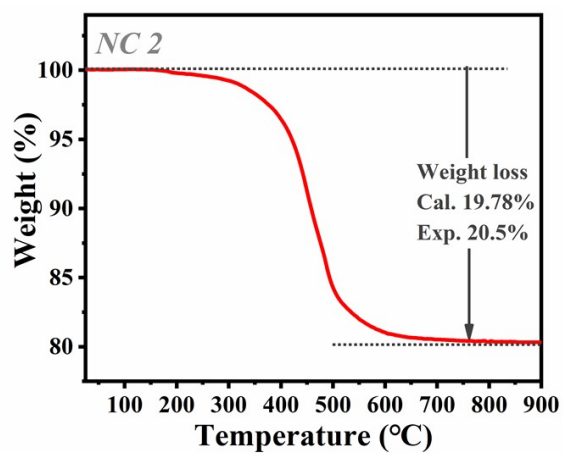


Figure S4. TGA curve of NC 2.

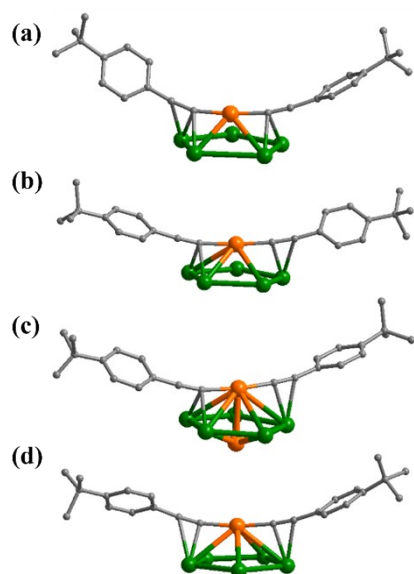


Figure S5. Four different kinds of binding motifs of surface “Bu-PhC≡C-Au-C≡CPh-’Bu” staple units on the Ag₅ faces of the Ag₂₀ shells in NC 1. Color labels: Au, orange; Ag, green; C, gray. All hydrogen atoms are omitted for clarity.

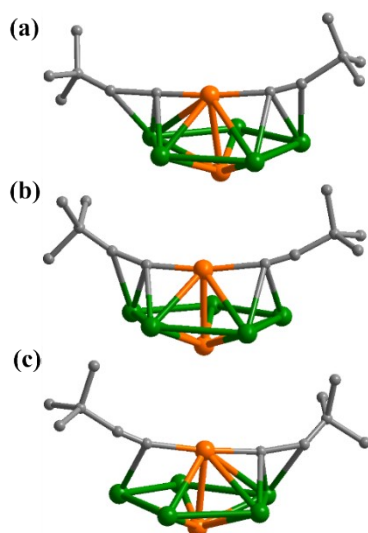


Figure S6. Three different kinds of binding motifs of surface “BuC≡C-Au-C≡C’Bu” staple units on the Ag₅ faces of the Ag₂₀ shells in NC 2. Color labels: Au, orange; Ag, green; C, gray. All hydrogen atoms are omitted for clarity.

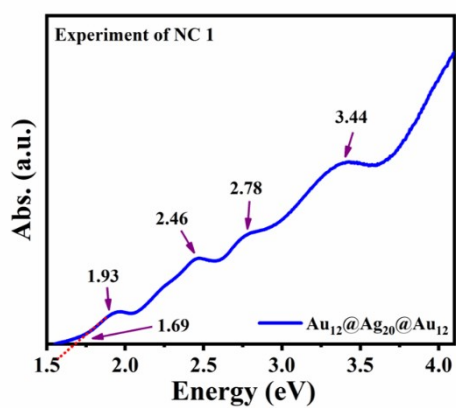


Figure S7. The optical absorption of NC 1 with X axis plotted as energy.

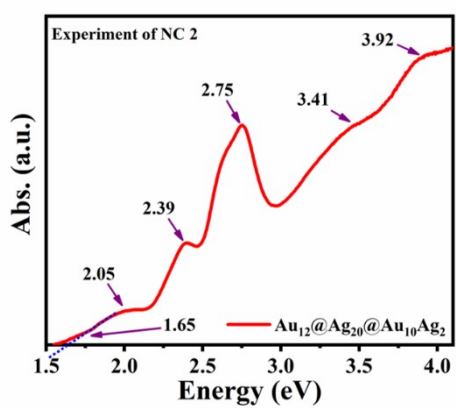


Figure S8. The optical absorption of NC 2 with X axis plotted as energy.

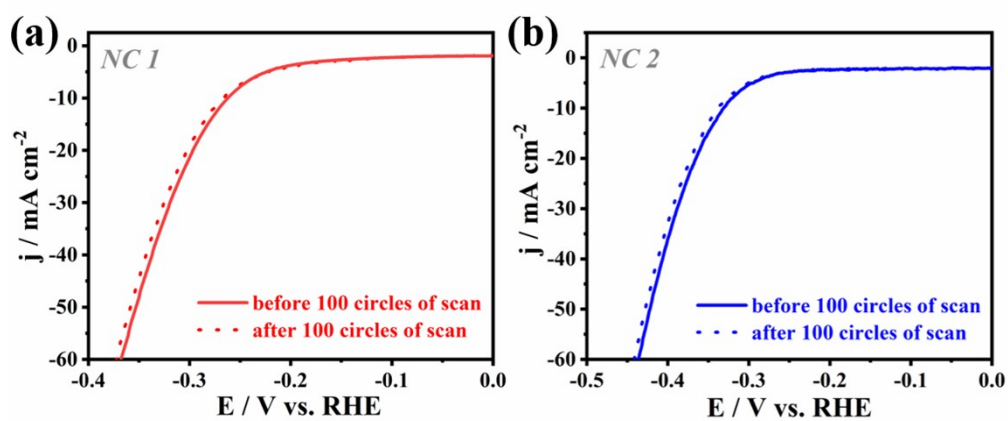


Figure S9. The enlargement of HER polarization curves of (a) NC 1 and (b) NC 2 catalysts before and after 100 circles of scan.

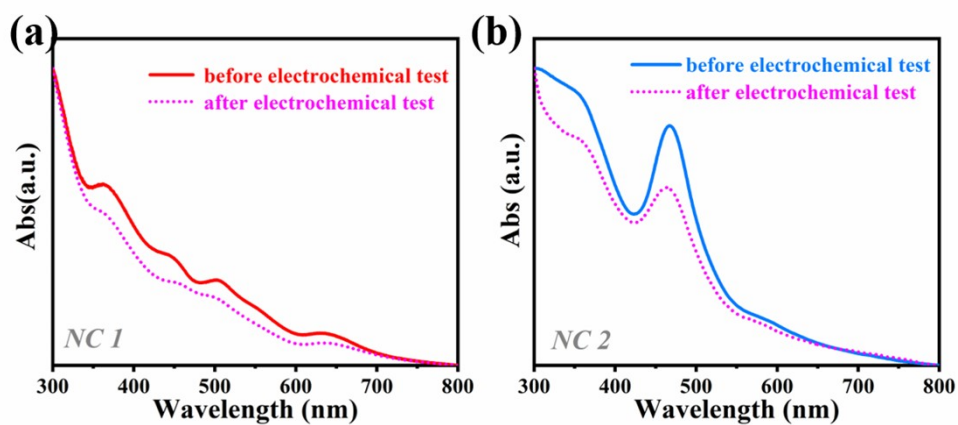


Figure S10. The absorbance spectra comparison of (a) NC 1 and (b) NC 2 before and after electrochemical test.

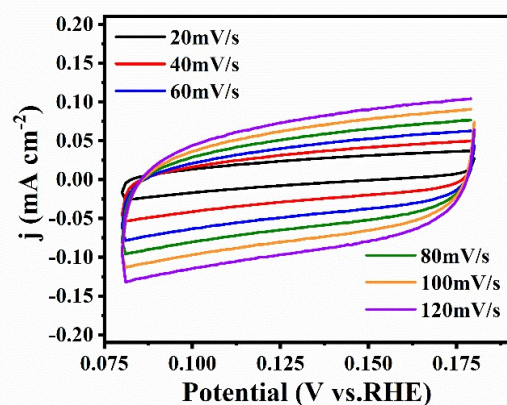


Figure S11. CV curves of NC 1 between 0.08 and 0.18 V vs. RHE with different scan rates (20, 40, 60, 80, 100, and 120 mV·s⁻¹).

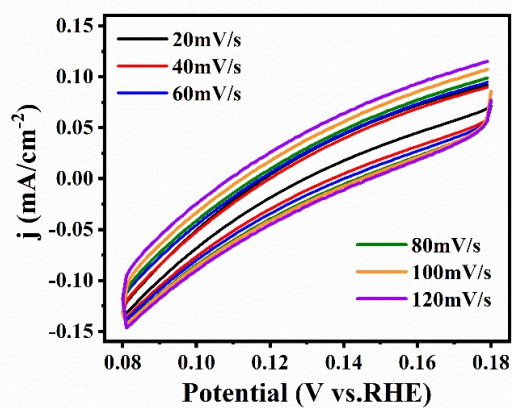


Figure S12. CV curves of NC 2 between 0.08 and 0.18 V vs. RHE with different scan rates (20, 40, 60, 80, 100, and 120 mV·s⁻¹).

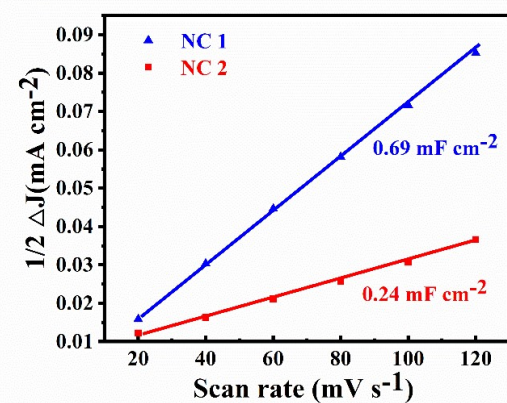


Figure S13. The dependence of capacitive current and scan rate.

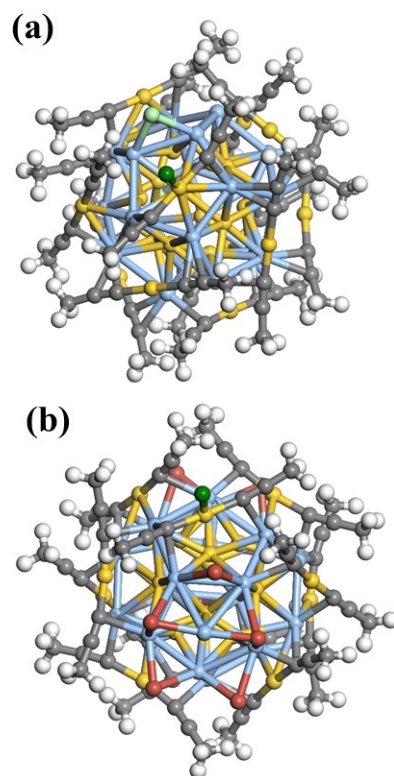


Figure S14. The adsorption structures of *H on the (a) NC 1 and (b) NC 2. Color legend: Au, gold; Ag, blue; C, gray; Cl, cyan; Br, red; *H, green; other H, white. All hydrogen atoms are omitted for clarity.

Table S1. The crystal structure parameters for NC 1.

Identification code	NC 1	
Empirical formula	$C_{288}H_{312}Ag_{20}Au_{24}Cl_2, H_2O$	
Formula weight	10746.87	
Temperature	100.00(10) K	
Crystal system	Monoclinic	
Space group	P 1 21/n 1	
a	21.06600(10) Å	$\alpha = 90^\circ$
b	32.5271(2) Å	$\beta = 98.5530(10)^\circ$
c	45.5844(3) Å	$\gamma = 90^\circ$
Volume	30887.8(3) Å ³	
Z	4	
Calculated density	2.311 mg·m ⁻³	
Absorption coefficient	31.190 mm ⁻¹	
F (000)	19680	
Crystal size	0.13 × 0.07 × 0.07 mm ³	
Radiation	MoK α ($\lambda = 0.71073$)	
2 θ range for data collection	2.385 to 76.903°	
Index ranges	$-22 \leq h \leq 26, -38 \leq k \leq 40, -56 \leq l \leq 57$	
Reflections collected	237255	
Independent reflections	61867 [R(int) = 0.0609]	
Data/restraints/parameters	61867 / 0 / 415	
Goodness-of-fit on F ²	1.092	
Final R indexes [$I \geq 2\sigma(I)$]	$R_1 = 0.0735, wR_2 = 0.1811$	
Final R indexes (all data)	$R_1 = 0.0869, wR_2 = 0.1913$	
Largest diff. peak/hole	5.600/ -2.914 e Å ⁻³	

Table S2. The crystal structure parameters for NC 2.

Identification code	NC 2	
Empirical formula	$C_{96}H_{144}Ag_{22}Au_{22}Br_{3.28}Cl_{2.72}$	
Formula weight	8362.42	
Temperature	149.99(11) K	
Crystal system	Monoclinic	
Space group	C 1 2/m 1	
a	16.1655(6) Å	$\alpha = 90^\circ$
b	22.070(2) Å	$\beta = 115.255(4)^\circ$
c	28.0809(16) Å	$\gamma = 90^\circ$
Volume	9060.9(11) Å ³	
Z	4	
Calculated density	3.156 mg·m ⁻³	
Absorption coefficient	20.833 mm ⁻¹	
F (000)	7572	
Crystal size	0.45 x 0.3 x 0.25 mm ³	
Radiation	MoK α ($\lambda = 0.71073$ Å)	
2 θ range for data collection	2.883 to 29.000°	
Index ranges	$-38 \leq h \leq 38, -30 \leq k \leq 17, -15 \leq l \leq 22$	
Reflections collected	29205	
Independent reflections	12003 [R(int) = 0.0453]	
Data/restraints/parameters	12003 / 1170 / 586	
Goodness-of-fit on F ²	1.049	
Final R indexes [$I \geq 2\sigma(I)$]	$R_1 = 0.0824, wR_2 = 0.2157$	
Final R indexes (all data)	$R_1 = 0.1247, wR_2 = 0.2576$	
Largest diff. peak/hole	3.118/ -2.655 e Å ⁻³	